RSC Advances

ROYAL SOCIETY OF CHEMISTRY

www.rsc.org/advances

Cite this: DOI: 10.1039/c0xx00000x

www.rsc.org/xxxxxx

ARTICLE TYPE

Effect of solvent on the uncatalyzed synthesis of aminosilane-functionalized graphene

Muhmmad Z. Iqbal,[a,b] Marios S. Katsiotis[a] , Saaed M. Alhassan[a], Matthew W. Liberatore[b] and Ahmed A. Abdala*[a]

Received (in XXX, XXX) Xth XXXXXXXXX 20XX, Accepted Xth XXXXXXXXX 20XX
DOI: 10.1039/b000000x

Uncatalyzed functionalization of thermally reduced graphene (TRG) with 3-aminopropyltriethoxy silane (APTS) is reported and the effect of the solvent on selective functionalization is discussed. The chemical, morphological and thermal properties of the functionalized TRG (f-TRG) have been studied using FTIR, XPS, EELS, Raman spectroscopy, TEM, and TGA. Our results indicate that the use of organic solvent during the silylation reaction not only increases grafting yield from 7 to 8 atomic% of Si attachment but also directs APTS groups to the edges of TRG as revealed using energy filtered TEM elemental mapping. A reaction mechanism based on attachment of the silane groups on TRG surface through residual, surface bound phenolic and carbonyl groups is proposed and discussed. The present approach provides an economical route for mass production of APTS-f-TRG and opens up a shed lights on the role of organic solvents in silane functionalization of graphene.

Introduction

Since its discovery in 2004, graphene has attracted the attention of researchers owing to its extraordinary electronic, thermal and mechanical properties[1-5]. Due to this combination of extraordinary properties in addition to the very high surface area, graphene is widely used as a nano-filler in manufacturing of polymer nanocomposites with improved mechanical, thermal and electrical properties[6-10]. Nevertheless, homogenous dispersion of graphene and strong interfacial interactions between graphene and the polymer matrix is required to obtain enhanced properties. The chemical functionalization of graphene alters the Van der Waals interactions among the nanofiller aggregates, making them easier to disperse in a polymer matrix and can also enhance the interface between graphene and the polymer matrix. On the other hand, the extremely high surface area of graphene makes it an ideal candidate as an adsorbent for H_2 storage[11], removal of pollutants from water[12], oil[13], and gases[14]. In order to enhance the compatibility of graphene with polymer matrices and increasing its adsorption affinity functionalization of graphene may be required.

The use of residual oxygen pendent groups on thermally or chemically reduced graphene for further attachment of the organic moieties is an attractive route exploited for covalent functionalization of graphene[15]. Silane coupling agents are historically applied to surface modification of nanofillers[16-20]. Graphene produced from reduction of graphite oxide contains sufficient amounts of hydroxyl, epoxy and carboxyl groups on their basal planes and edges[21]. These groups can be dehydrated with silane coupling agents under appropriate conditions. Also, the functional groups of silane coupling agents can be chemically attached to the polymer. Amongst, 3-aminopropyltriethoxysilane (APTS) has been widely reported as a reactive coupling functionalization for CNTs[17, 22] and graphene[18, 19, 23]. Specifically, Wang et al. reported attachment of APTS on graphene surface and used the functionalized graphene in graphene-epoxy nanocomposites[18]. The grafting of APTS was proposed to follow dehydration of carboxylic and hydroxyl groups. In another report by Yang et al., APTS reaction with chemically converted graphene resulted in 4% Si grafting on atomic basis[19]. However, the proposed mechanism of APTS grafting was through the epoxide groups on the graphene surface. In addition, both reports employed DCC catalyst to accelerate reaction kinetics and enhance the grafting yield. A 3.4 atomic% Si yield has also been reported for graphene by Ganguili et al.[23]. Gasper et al. reported detailed reaction mechanism for grafting various types of silanes on CNT[22]. Therefore, these studies outline the importance of silane functionalized graphene in various applications. For the mass production of APTS-f-graphene, a method that does not utilize a catalyst is needed. Catalyst can increase the production cost by many fold. Hence, a catalyst-free method in functionalizing graphene by silane based coupling agents is highly desirable. In addition, in order to use the APTS-f-graphene in different applications, a better understanding of APTS chemistry is needed. This study focuses on the above mentioned question using various characterization techniques.

In the present work, we present a catalyst-free method for APTS attachment on TRG with higher yield of silane grafting. Thermally reduced graphene (TRG) is produced via simultaneous

thermal exfoliation and reduction of graphite oxide (GO). The effect of solvent on the localization of functionalization on graphene surface is also discussed. Two simple routes for reacting APTS with TRG are presented; 1) using toluene as a solvent, and 2) using pure silane in absence of solvent. A mechanism for APTS attachment onto graphene that reflect the effect of organic solvent on functionalization chemistry is proposed and supported by the results of various characterization tools to. The resulting functionalized graphene was thoroughly characterized using physicochemical methods to understand the nature of functionalization reaction. The success of the simple reaction routes is expected to promote mass production of APTS-functionalized graphene.

Experimental details

Natural flake graphite (-10 mesh, 99.9%, Alfa Aesar), Sulfuric Acid (95-97%, J.T. Bakers), Hydrochloric Acid (37%, Reidel-deHaen), Hydrogen Peroxide (30% solution, BDH), Potassium Permanganate, Sodium Nitrate (Fisher Scientific), 3-aminopropyl triethoxysilane (98%, Merck) and toluene (99.5%, Panreac) were used as received.

Preparation of TRG

TRG was produced via the thermal exfoliation of graphite oxide (GO)[24]. In this method, graphite is oxidized using Staudenmaier method[25] as follows: graphite (5 g) was placed in ice-cooled flask containing a mixture of H_2SO_4 (90 ml) and HNO_3 (45 ml) then potassium chlorate (55 g) was slowly added to the pre-cooled (0-5° C) reaction mixture under stirring. After the reaction proceeds for 96 h, it was stopped by pouring the reaction mixture into water (4 L). GO was filter and washed with HCl solution (5%) until no sulfite ions were detected. Finally, the resulting deep brown colored mixture was repeatedly washed with copious amount of water until no chloride ions was detected. The wet GO was dried under vacuum overnight. TRG was made by rapid heating of dry GO powder at 1050° C in a tube furnace (Model 21100, Barnstead Thermolyne) under flow of nitrogen for 30 s.

Silylation reaction

Two simple routes were used to examine the solvent effect on the mechanism of APTS attachment.

Method 1: 50 mg of TRG was dispersed in 30 mL of pure APTS in a 50 mL reaction flask. The mixture was refluxed at 100° C for 3 hours under stirring then cooled to room temperature and the functionalized TRG (f-TRG) was recovered by vacuum filtration.

Method 2: same as Method 1 except the 30 mL of pure APTS was replaced by 50 mL of 30 vol% APTS in toluene. TRG functionalized using this method is denoted (f-TRG_S).

To remove any physically adsorbed APTS from the surface of TRG, f-TRG was dispersed in toluene under stirring for 15-20 minutes followed by tip-sonication for additional 5 minutes and filtering under vacuum. To ensure the complete removal of any unreacted APTS, this washing procedure was repeated twice. The samples were then dried in air at 120° C for 2 h.

Characterization

Transmission Electron Microscopy (TEM) analyses were performed using FEI Tecnai G20 with 0.11 nm point resolution and operated at 200 kV. Electron Energy Loss Spectroscopy (EELS) was performed using post column energy filtered camera (Gatan GIF 963). Energy filtered TEM (EFTEM) mapping was applied to map the location of the elements on the surface of f-TRG samples by measuring core, post-edge and pre-edge losses of the respective elements using the "three-window method" technique[26]. X-ray Photoelectron Spectroscopy (XPS) measurements were performed using SSX-100 system (Surface Science Laboratories, Inc.) equipped with a monochromated Al Kα X-ray source, a hemispherical sector analyzer (HSA) and a resistive anode detector. For the high-resolution spectra, the lowest binding energy C1s was set at 285.0 eV which was used as the reference for all of the other elements. Fourier Transformed Infrared (FTIR) spectra of TRG, f-TRG_p, and f-TRG_s in the range of 400-4000 cm^{-1} were collected using Thermo Nicole FTIR at a resolution of 4 cm^{-1} and 32 scans. The spectra of the dried samples were obtained in KBr pellets (Merck, spectroscopic grade) containing 0.2 wt% of TRG. A LabRAM HR (Horiba Scientific) was used to obtain Raman spectra. Typically, a 50x objective was used with 633-nm excitation line. Thermo-gravimetric analysis was carried out by STA coupled with a mass spectrometer (STA-QMS, 409 PC Netzsch). The temperature range was from 35 °C to 450 °C at a ramp rate of 10 °C in an inert atmosphere of nitrogen (30 mL/min). The electrical conductivity was measured by a custom-made conductivity cell at the National Renewable Energy Laboratory (Golden, CO). The samples were bath-sonicated in 10 mL of water/isopropanol solution (3/1) followed by 2 minutes of tip-sonication. The dispersed samples were dried on copper stubs for the conductivity measurements. The resistivity was measured using a multimeter (Waveteck 28XT, Accuracy: ±1% + 0.1 Ohm). Further details on experimental procedures are provided in the supporting information.

Results and discussion

The simultaneous thermal exfoliation and reduction of GO to TRG was successfully confirmed by XRD and TEM (see supporting information Fig. s1).

The APTS-functionalized TRG was systematically characterized to investigate the effect of the solvent on the chemical, thermal, electrical and morphological properties of APTS-f-graphene. The chemical nature of the f-TRG is studied by FTIR, XPS, Raman, and electron energy loss (EEL) spectroscopy to elucidate the mechanism of APTS grafting on TRG. TEM micro-images and elemental mapping were used to study the morphology of f-TRG. The electrical conductivity and thermal stability of f-TRG are also discussed.

Chemical analysis

FTIR spectroscopy (Figure 1) confirms the successful attachment of APTS on TRG by the appearance of additional functional group stretches associated with APTS-TRG linkages. The intensity of peak D (1189 cm^{-1}), which corresponds to –COOH groups has been reduced. This suggests that the carboxylic groups are among the active moieties for APTS attachment. Peak H (1544 cm^{-1}), which corresponds to C=C aromatic carbons stretching in non-graphitic domains, remains the same for f-TRG_P but shifts to a higher frequency (~1558 cm^{-1}) for f-TRGs. The

shift to higher frequency for TRGs suggests the possibility of APTS reacting with C-hexagons of the TRG sheets in addition to the reaction with TRG's functional groups (Also confirmed by XPS analysis). The carbonyl group > C=O at ~1740 cm^{-1} (peak J) also remains the same for pure and f-TRG. The appearance of new peaks in f-TRG_P and f-TRG_S is attributed to –Si-O stretching [peak A (–Si-OH at 914 cm^{-1}), peak B (Si-O-Si at 1015 cm^{-1}) and peak C (–Si-O-R at 1110 cm^{-1})], indicating the covalent functionalization of graphene. The effect of the solvent is demonstrated by the broadening of Si bonding peaks and the appearance of -Si-O-Si- peaks, which suggests session of the alkyl group and crosslinking of multiple APTS molecules. This may be attributed to the ability of toluene to transfer free radical to APTS in a similar manner to its chain-transfer effect during polymerization of monomers such as styrene. Also, the NH-amine vibration, which is expected around 3300-3400 cm^{-1} in f-TRG (peak M), is not prominent, likely due to overlapping with the characteristic bands of adsorbed water in the same region[19]. Peak F (1380 cm^{-1}) corresponds to in-plane –OH deformation and peak G (1485 cm^{-1}) is assigned to phenyl groups. The –NH bending vibration mode[27] (peak I at 1629 cm^{-1}) also confirms the direct attachment of amine groups to graphene and its very low intensity indicates the presence of a very small amount of this sequence. Moreover, the appearance of two new peaks at ~2853 and 2925 cm^{-1} for the f-TRG samples is attributed to CH_2-CH_2 symmetric and asymmetric vibrations from APTS[22].

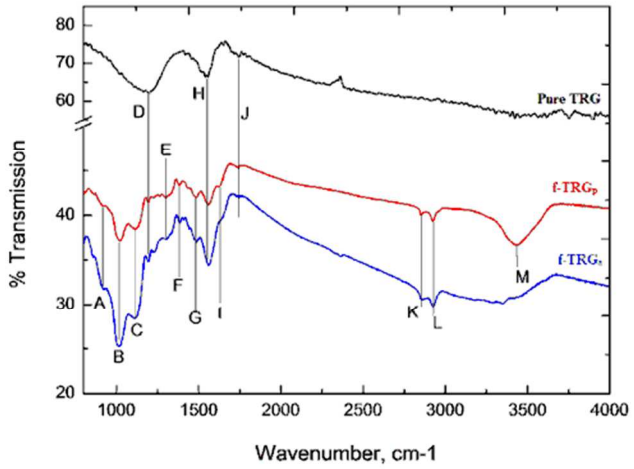

Fig. 1 FTIR spectra of the pure and f-TRGp and f-TRGs

While FTIR confirmed the attachment of APTS to graphene, a quantitative estimate of the level of functionalization is provided by XPS analysis. The results shown in Table 1 reveal that the functionalized graphene samples contain 7.4% Si and 6.9% N for f-TRG_P and 8.0% Si and 6.5% N for f-TRG_S. Not only we are able to achieve such high yield without the use of any catalyst but also the observed yield is higher than all previously reported for nanocarbons, e.g., graphene oxide[19] and CNT[22]. The Si/N ratio for f-TRG_P is close to the stoichiometric APTS ratio of 1. However, The Si/N ratio for f –TRG_S is 1.2. A Si/N atomic ratio greater than unity suggests the session of the amino branch from APTS induced possibly by solvent induced radical transfer to carbon atoms in the amino branch of APTS, which was also suggested by the FTIR analysis.

Table 1 Atomic composition of pure and f-TRG as obtained from XPS

	Atomic%			
	C	O^{1s}	N^{1s}	Si^{2p}
TRG	89.1	10.9	-	-
f-TRG_P	66.8	20.0	6.9	7.4
f-TRG_S	67.4	18.2	6.4	8.0

In order to further explore the structure of f-TRG, high resolution C^{1s}, O^{1s}, N^{1s} and Si^{2p} spectra were collected (Figure 2 and Table 2). In C^{1s} spectra, all the samples exhibit the same graphitic C=C peak whose area percentage decreases in the f-TRG due to the appearance of new bands. The C-O peak [19] in TRG decreased in f-TRG_P and f-TRG_S samples. Due to the smaller electronegativity difference between C and N compared to between C and O, the peak for C-N is observed at a lower binding energy (BE). The relative percentage of ~285 eV peak has increased significantly in f-TRG_P and f-TRG_s. The peak for C=O carboxylic groups for f-TRG_S has a reduced intensity compared to the C=O peak in TRG, it vanishes in f-TRG_P. Thus, C=O is a potential attachment site for APTS on TRG (i.e, the carboxylic group on TRG). The disappearance of C=O in f-TRG_P suggests selective attachment of APTS onto the carboxyl group. Meanwhile, two additional peaks are observed in C^{1s} spectra of f-TRG_P. The first peak at 286.16 eV is assigned to aliphatic C-N group[19, 28] whereas the second peak at 288.85 eV is attributed to either N-C=O or O-C=O[22]. Since APTS is a bi-functional silane, its grafting to TRG can also take place through a linkage between the amine group in APTS and the carbonyl or carboxylic functionalities on TRG. The small peak at 288.85 eV BE is attributed to such linkage[22]. However, the relative area of this peak is very small indicating that fraction of APTS that attaches to TRG through the amine linkage, is relatively small. Therefore, we conclude that APTS reacts bi-functionally with TRG through attacking the phenolic and carbonyl groups on the surface. Moreover, the π-π* interactions[18] are observed in TRG and f-TRG_S whereas no π-π* interactions are observed in f-TRG_P possibly due to the disappearance of C=O peak in f-TRG_P.

Unlike C^{1s} core level, where the assignment of the peaks to single and multiple C–O bonds is quite straight forward, the assignment of O^{1s} peaks is more difficult. The carbonyl groups C=O are expected between 531 and 532 eV, C–O bonds in ethers and hydroxyls between 532 and 533.5 eV, whereas ether oxygen atoms in esters and anhydrides appears at 533.8–534.6 eV, or higher, and the carboxilates should originate a single component at BE similar to that of C=O groups in the case of oxidized carbon surfaces. Although C=O is observed for TRG, f-TRG_P and f-TRG_S, the relative intensity of C=O is lower in the f-TRG samples as a result of APTS attachment in agreement with the analysis of the C^{1s} spectra. The C-O-C/O-C=O band in TRG appears at higher BE for TRG_s showing the bonding with a more electronegative structure at this point. The peak at ~533.5eV originates from $O^{\delta-}$ contribution of TRG due to the presence of O^{-2} ions.

The appearance of new Si-O bands in f-TRG_P and f-TRG_S is sign of APTS functionalization and its intensity and relative contribution depend on the degree of APTS functionalization[29]. Moreover, the carboxylic band observed for TRG at ~534 eV disappears in the f-TRG samples in excellent agreement with the results from C^{1s} XPS spectra and FTIR.

Cite this: DOI: 10.1039/c0xx00000x

www.rsc.org/xxxxxx

ARTICLE TYPE

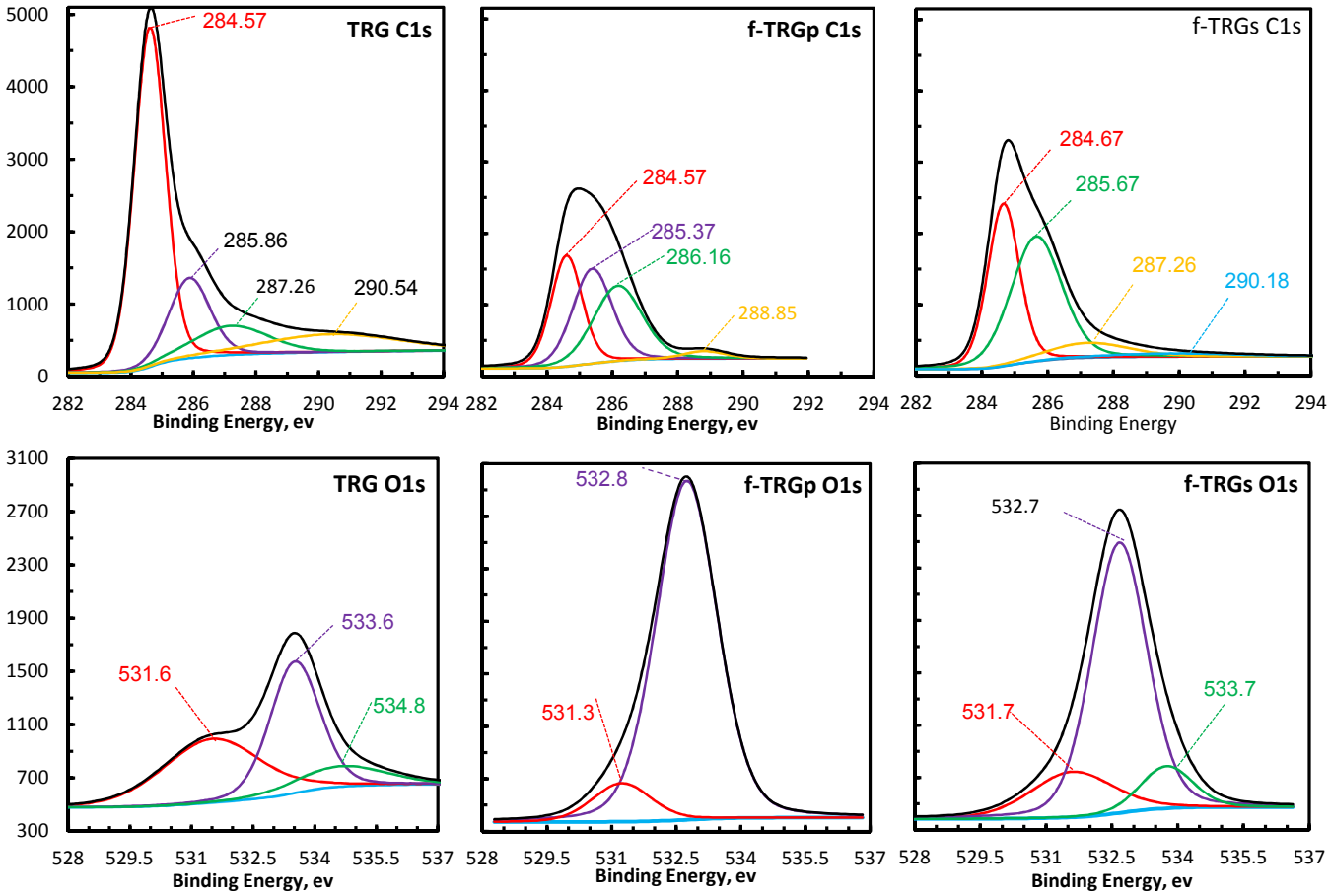

Fig. 2 High resolution XPS spectra of pure and f-TRG samples. Y-axis scale for all C1s spectra is the same and Y-axis scale for all O1s spectra is the same

Table 2 High resolution fitting of C^{1s} and O^{1s} groups appearing in the XPS spectra of TRG, f-TRG_p, and f-TRG_s

	C^{1s}						O^{1s}			
	C=C (sp^2)	C-O/ C-N	C-N	C=O	N-C=O/ O-C=O	π-π*	C=O	Si-O	C-O-C/ O-C=O	O-C=O
TRG	284.57	285.86	-	287.26	-	290.54	531.56	-	533.55	534.84
f-TRG_p	284.57	285.37	286.16	-	288.85		531.26	532.75	-	-
f-TRG_s	284.67	285.67	-	287.26	-	290.14	531.66	532.65	533.74	-

The prominent changes in O^{1s} spectra of the pure and functionalized samples clearly indicate that the silanization has changed the structure of the graphene sheets. Table 2 summarizes the results of the high resolution C^{1s} and O^{1s} spectra. Furthermore, the details of high resolution N^{1s} and Si^{2p} XPS spectra of f-TRG are provided in the supplementary information. Considering the XPS data and the structure of f-TRG, the APTS may attach to graphene through the phenolic as well as the carbonyl surface groups where a similar mechanism has been reported by Gasper et al.[22] for CNTs. However, this multiple functionality may differ from the previously reported mechanisms for silylation where the aminosilanes are proposed to attack the epoxy groups[19] on the graphene surface. In addition, the second possibility of enhanced grafting efficiency of APTS is NH_2-silicon polymerization[22] on the surface of TRG

Previous reports demonstrated APTS grafting efficiency on MWCNT[22] up to 4.5 Si atomic%, and 3.4%[23] and 4.1% for graphene[19]. The current method is able to generate much higher yield of ~ 7.4% Si attachment in f-TRG_P and ~ 8% Si in f-TRG_S. The increase in Si attachment can be attributed to the reaction of APTS with not only the surface functionalities of graphene but also with the surface C-atoms. Schematics of possible

mechanisms are also discussed later.

The effect of silane attachment on the electronic structure of graphene is also confirmed by EELS. The core-level energy losses of C, O, N and Si (Figures 3-4) are measured at the areas of minimum overlapping between the graphene sheets. All collected EELS spectra are background corrected.

The carbon K-edge (Figure 3-a) is the characteristic of graphene[30]. The sp^2 hybridization of TRG is clearly observed as sharp peaks corresponding to the $1s\cong \rightarrow \pi^*$ and $1s \rightarrow \sigma^*$ transitions at 289 and 294 eV, respectively. Interestingly, the hybridization state of graphene is altered in the functionalized samples. In specific, the sp^2 structure becomes less dominant in the case of f-TRG_P and f-TRG_S in excellent agreements with FTIR, XPS and Raman results. The ratio $sp^2/(sp^2+sp^3)$ was calculated using the peak-ratio method[31] and found to be 98±1.5% , 94±1.1%, and 87±1.9% for TRG, TRG_p, and TRG_s, respectively. A plausible explanation for this change in hybridization is attributed to the sp^3 structure of carbon atoms in silane. Based on the current information obtained from FTIR and XPS on the successful grafting of APTS on graphene, the apparent change in hybridization most possibly represents the combination between the sp^2 structure of graphene and the sp^3 structure of silane. The oxygen K-edge region is presented in Figure 3-b and exhibits an overall shape equivalent to that of the N K-edge. Two π^* peaks can be observed at 530 and 535 eV which are attributed to the C-O bonds. The dominating structure however, is the absorption beyond 541 eV with a particular triangular shape. Similar findings were observed in literature[32, 33] and the aforementioned structure was attributed to the increased presence of Si-O bonds originating from the APTS-attachment on graphene.

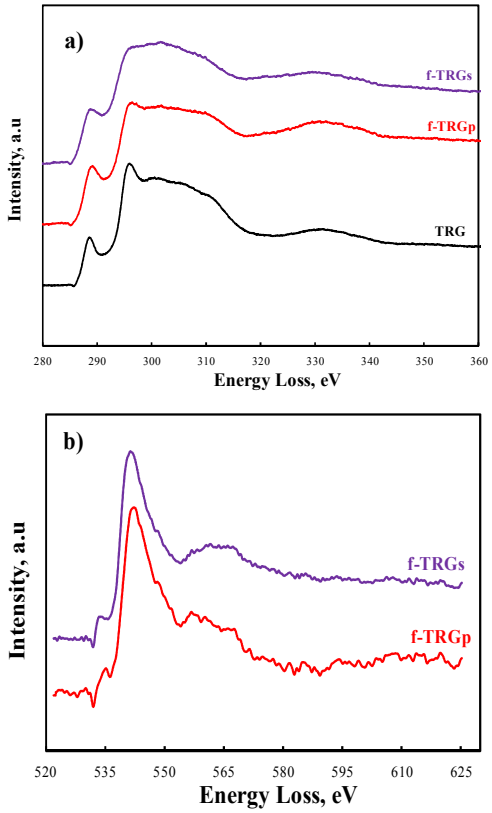

Fig. 3 EELS Carbon K-edge a), and Oxygen K-edge b)

Figure 4-a displays the nitrogen K-edge evolution, where a strong π^* absorption is observed at ~399 eV and a structure-less σ^* absorption of triangular shape is observed at ~410 eV.

The π^*-transition is usually attributed to unsaturated C-N bonds[34]. Since this type of bonds is not present in the silane molecule, the peak at ~399 eV can be attributed to a possible loose attachment of the amine part of silane on the graphene surface in agreement with FTIR and XPS spectra. Regarding the σ^* absorption, this can be attributed in the Si-N bond present in APTS. In the case of silicon L-edge (Figure 4-b), the EELS spectra from the functionalized samples are very similar to the spectrum of silicon oxide[35]. Peak at 99 eV corresponds to elemental silicon (Si), at 105 eV to Si-N bond (Si^{1+}) and peaks at 108 and 116 eV to Si-O (Si2+) and Si=O (Si^{4+}) bonds respectively[36, 37]. Regarding Si L_1 edge at ~155eV, strong overlapping with the threefold L_{2-3} edge prevents the acquisition of any useful information. Regardless, silicon EELS strongly supports the presence of silane grafted on graphene.

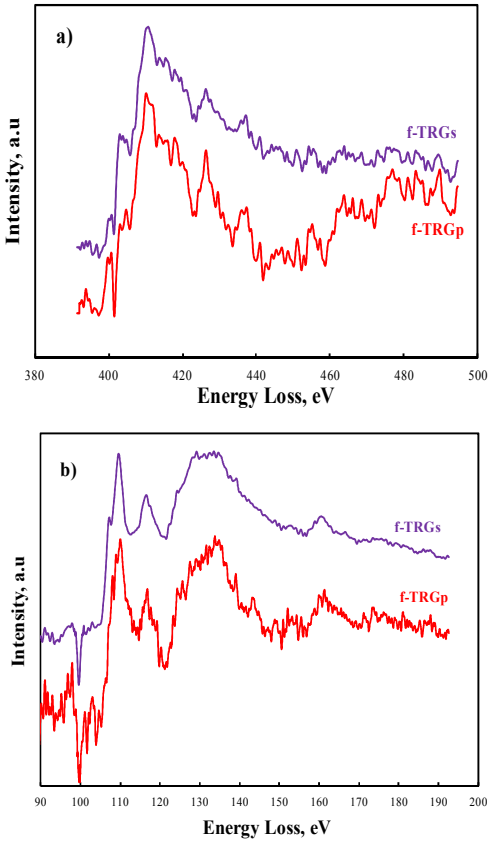

Fig. 4 Nitrogen K-edge a) and Silicon L2-3-edge b)

The effect of APTS functionalization and the degree of exfoliation in TRG was also examined by the Raman spectroscopy (Figure 5), which is known for its unambiguous nondestructive identification[38]. For graphitic materials, the typical Raman bands are: a defect-induced D band at 1350 cm^{-1}, an in-plane vibration of sp^2 carbon at 1580 cm^{-1} (G band), and a two-phonon double-resonance process at ca. 2700 cm^{-1} (2D band). The G-band position increases with decreasing number of layers in graphene[39]. Herein, the G band centred at 1770 cm^{-1} for TRG has been upshifted to 1778 cm^{-1} on functionalization (Figure 5-a), thus revealing the decrease in the layer stacking[40], mainly due to

the presence of APTS. Moreover, compared to TRG (Figure 5b), the characteristic 2D band for f-TRGs and f-TRG$_P$ is observed to be blue shifted by about 28 cm^{-1} and accompanied with peak broadening, confirming that the functionalization lead to better exfoliation of TRG and formation of few-layer graphene flakes[41]

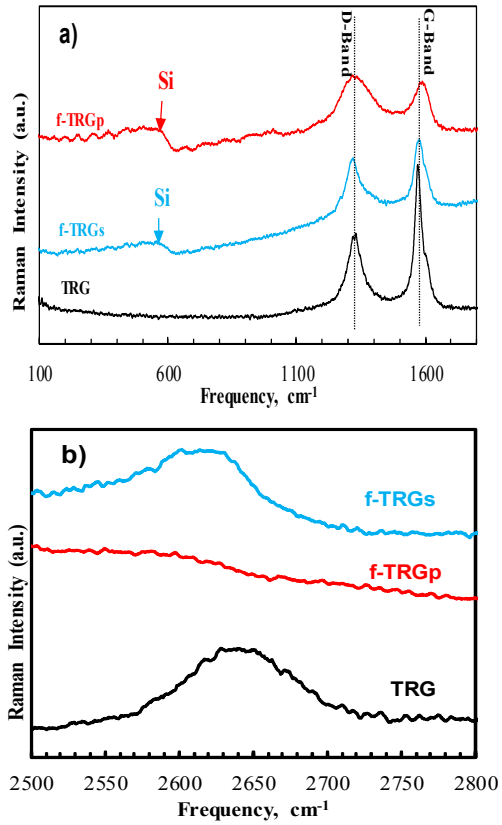

Fig. 5 Raman spectra of TRG samples a) D and G band and b) 2G (G') band

Additionally, the appearance of D peak at 1339 cm^{-1} has been attributed to the presence of structural disorder[42]. The D band arises from the activation in the first order scattering process of sp3 carbons in graphene, and the intensity ratio of D and G bands (I_D/I_G) expresses the sp^2/sp^3 carbon ratio, a measure of the extent of disorder[43]. The I_D/I_G for f-TRG$_S$ and f-TRG$_P$ has increased from 0.677 for TRG to 0.903 and 1.026, respectively. The increased I_D/I_G ratio is consistent with the functionalization of graphene through covalent bonding[44, 45] and also in agreement with the EELS results. In addition, the appearance of a new peak at lower frequencies between 500-600 cm^{-1} is ascribed to the Si grafting on TRG [46]. Hence, overall the Raman findings confirm the successful functionalization of TRG and the exfoliation state of TRG remains unaffected by APTS attachment.

Morphological analysis

TEM and EELS analyses are performed in order to understand the effect of functional moieties on the morphology of graphene and to define the bonding between APTS and TRG which can arise due the presence or absence of organic solvent. Pure TRG is composed of very thin sheets with lateral dimension from 0.5 to 1.5 µm (Figure 6). These thin sheets are composed of overlapping graphene layers; the sheets are well defined and separated. The inset in Figure 6-a shows a selected area electron diffraction (SAED) pattern collected from the center of the image, which verifies the crystallographic identity of graphene.

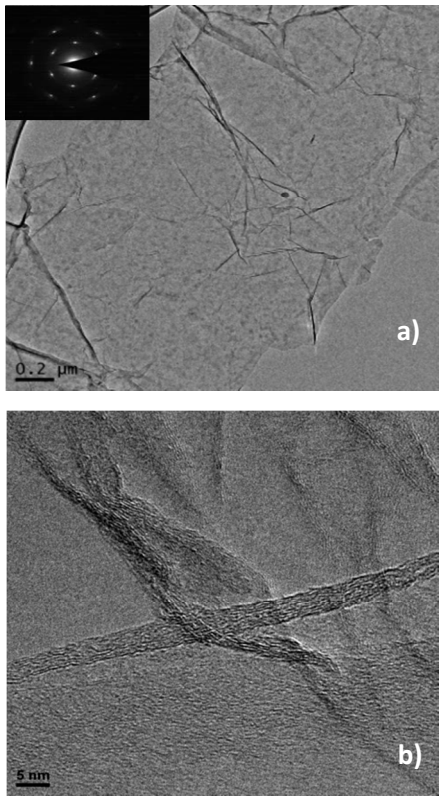

Fig. 6 TEM images of (a) pure TRG particle composed of overlapping graphene sheets (inset: SAED pattern from the center of the graphene particle), (b) HRTEM image of two overlapping graphene sheets

The High resolution TEM imaging (HRTEM) performed in areas where graphene was "folded", showed the presence of multi-layer structure with number of layers between 5 and 10. It worth noting that TEM does not provide any statistically significant estimate of the thickness or number of layer of graphene but is used here as a to provide a qualitative comparison between TRG and f-TRG. Finally, EDS results indicate the presence of a small amount of chlorine impurity (< 0.5%), probably originating from the HCl washing (see supporting information).

Although f-TRGp exhibits a structure similar to that of pure TRG, however, the sheets do not appear as well separated as were in the pure TRG (Figure 7). The silane creates defects in the graphene sheets (tears on the graphene surface) (see Figure 7-a for f-TRGp). On the other hand, no considerable change in the morphology of graphene sheets was observed for f-TRGs. Instead, the sheets are very well defined and separated, (Figure 7-b). The solvent appears to soften the severe attack of APTS on graphene and hinders breaking down of sheets to smaller ones. We infer that using organic solvent during the course of silane functionalization reaction helps in maintaining the intrinsic morphology of graphene. The EDS analyses (see supporting information, Table s2) from the two samples were in good agreement with the XPS elemental analysis: on average Si/N ratio is found to be equal to 1.05 for f-TRGp, and 1.25 for f-TRGs (average of EDS spectra collected at various points for each sample).

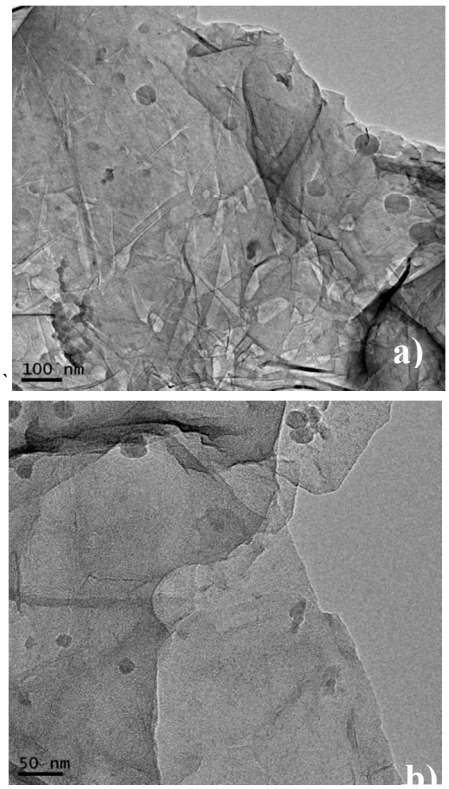

Fig. 7 TEM images of functionalized graphene ; (a) f-TRGp, (b) f-TRGs

Furthermore, in order to understand the preferable attachment sites for silane on TRG, EFTEM elemental mapping was performed on both f-TRG_p and f-TRG_S. To the best of our knowledge, there is currently no publication on EFTEM mapping of the functionalized graphene to determine the functionalization selectivity. However, the EFTEM elemental mapping, completed here (Figure 8), can be a simple and versatile method for studying the local functionalization. Bright spots in Figures 8-b, d represent Si from EFTEM Si-elemental mapping of Figures 8-a, c. It is interesting to note that, in f-TRG_P, Si (and N which is not shown here) is distributed over the entire graphene surface (Figure 8-b) representing a homogeneous distribution of the grafted silane on f-TRG_P surface. Thus, we infer that pure silane reacted homogeneously on the graphene surface. A small amount of localized Si is also observed on the sheet edge. Thus, the mode of silane grafting, when TRG is reacted with pure APTS, is with the surface functional groups as well as the functional groups on the sheet edges. On the other hand, in f-TRG_S, the Si is observed to localize on the sheet edges. The homogeneous surface distribution of Si was not observed as was seen in f-TRG_P. Thus, it appears that in the presence of organic solvents like toluene, the edge-functionalization of TRG can be the preferable mode of grafting. The selectivity of edge-functionalization might further be increased by choosing appropriate solvents and reaction conditions. In summary, solvent can play a vital role in the selective functionalization of TRG. Further studies will evolve better control on its chemistry for selective applications of silane functionalized TRG.

Based on the observations presented above, proposed reaction schemes for APTS with TRG are elucidated (Scheme 1). The TRG oxy-functionalities are distributed over the surface and sides of the sheets where the carboxylic groups are mainly located near the edges and most of hydroxyl and epoxy groups are distributed over the surface. In f-TRG_P, APTS reacts with most of the surface groups and there is less reaction with the side carboxylic groups..

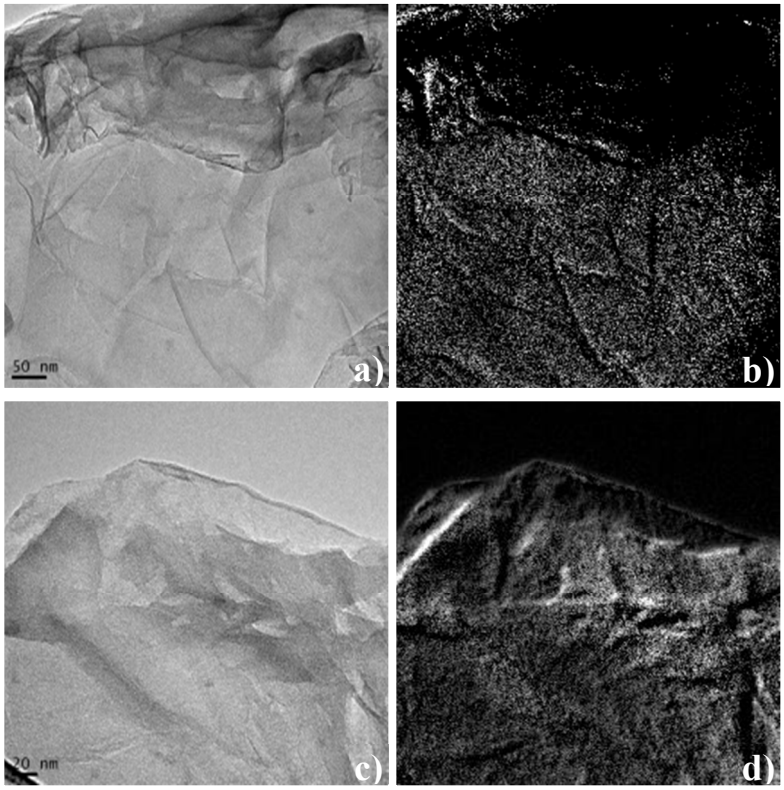

Fig. 8 TEM bright field image (a) and corresponding EFTEM maps of silicon (b) for f-TRGp; TEM bright field image (c) and corresponding EFTEM maps of silicon (d) for f-TRGs.

Cite this: DOI: 10.1039/c0xx00000x

www.rsc.org/xxxxxx

ARTICLE TYPE

In the case of f-TRG$_S$, the APTS molecules form covalent bonds with the carboxylic groups present on the sides of TRG sheets

The use of various solvents assisting silane functionalization is not uncommon. Toluene being a non-polar solvent with a dipole moment of 0.36 D has induced significant effects on the functionalization selectivity. Owing to the non-polarity of toluene and TRG being polar due to the presence of oxy-functional groups on its surface, the solvent helps assisting preferable distribution of silane on TRG surface; leading silane molecules to more reactive areas such as the edges. On the other hand, in the absence of solvent, the silane (being polar) is chemically adsorbed throughout the surface and edges. Increasing solvent polarity in silylation reaction been reported to decrease the rate of silylation of inorganic surfaces[47, 48]. Thus, using non-polar solvents such as cyclohexane, benzene, diethyl ether, chloroform,…etc can lead to interesting aspects for selective silane functionalization. Nevertheless, the probability and further quantification of the attached functional groups depending on other solvents is beyond the scope of this article.

Thermal stability and conductivity

The thermal characterization of the pure and f-TRG by TGA provides a reliable quantification of the relative amount of the introduced functionalities. As shown in Figure 9, both TRG$_P$ and TRG$_S$ have lower thermal stability compared to the pure TRG. The lower thermal stability of f-TRG samples compared to pure TRG is attributed to the full or partial detachment of the APTS groups from the graphene surface. The observed weight losses in the temperature range of 50-500° C are 16, 22, and 25% for TRG, f-TRG$_S$, and f-TRG$_P$, respectively.

As discussed in the previous section, the XPS results indicated that f-TRG$_P$ contains 7.4 atomic% Si, which corresponds to 15 wt.% APTS and f-TRG$_S$ contains 8 atomic% Si corresponding to 16 weight% APTS.

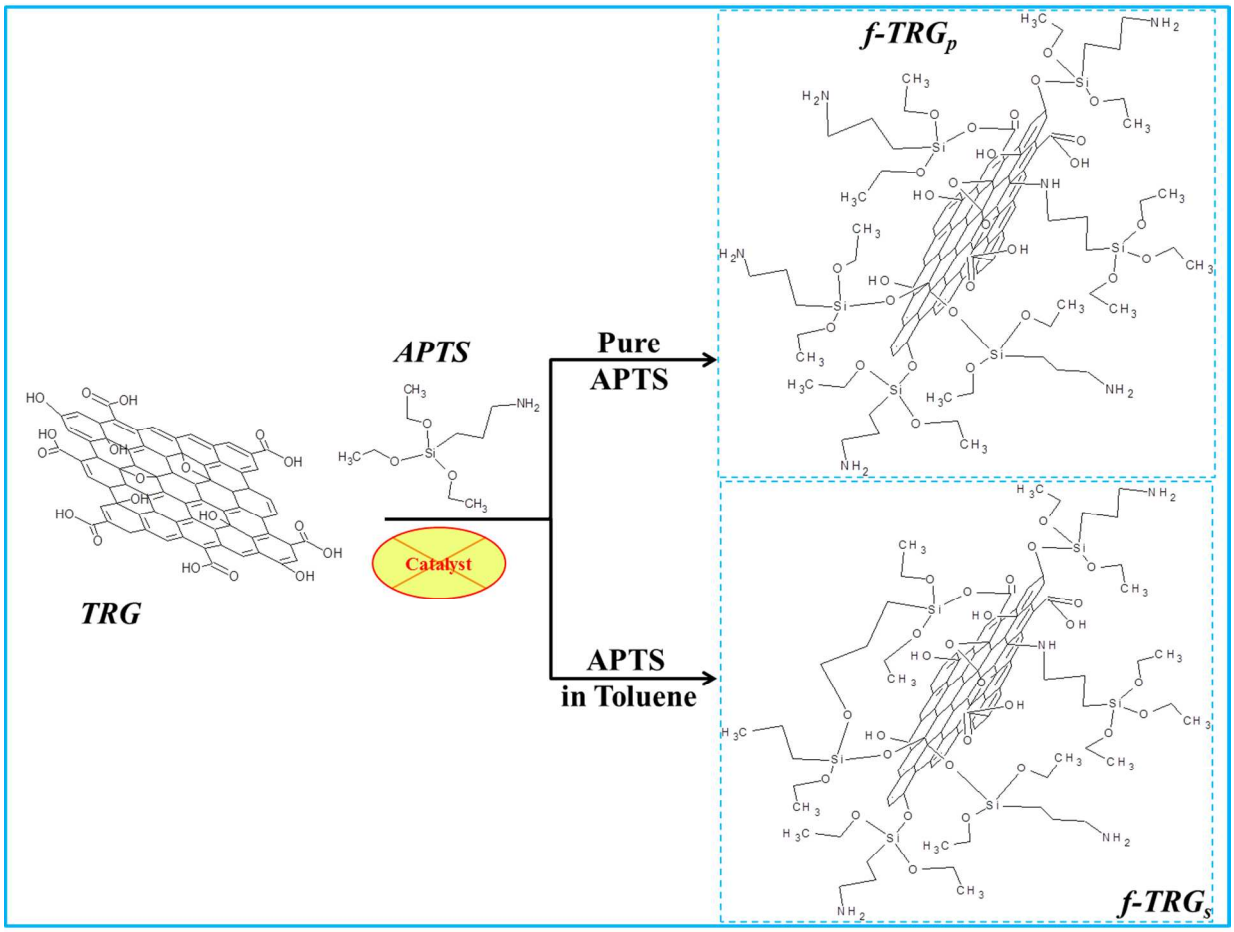

Scheme 1 Reaction of APTS with TRG. TRG contains carboxylic functionalities on the sides whereas hydroxyl and epoxy groups are mainly distributed over the surface

Cite this: DOI: 10.1039/c0xx00000x

www.rsc.org/xxxxxx

ARTICLE TYPE

Therefore, about 40% of APTS in f-TRGP and 55% of APTS in f-TRGS is lost between 50 and 500° C, respectively. Moreover, the higher weight loss for f-TRGS compared to f-TRGP might be due to the most of the attached silane groups on the edges (as observed from the elemental mapping), and in f-TRGP, the silane moieties are distributed over the surface and on the edges of the sheets. Thus, it can be inferred that the end-functional groups are thermally less stable as compared to the surface distributed labile groups.

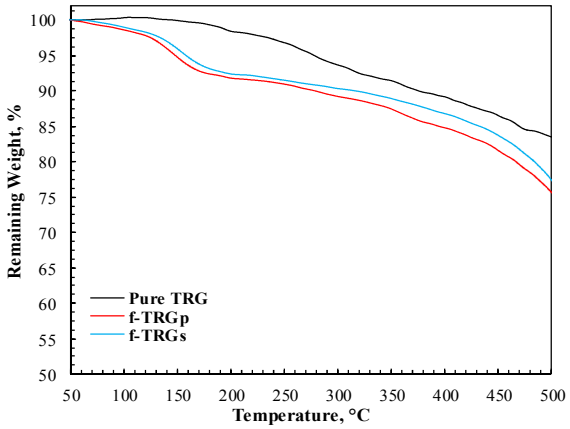

Fig. 9 Thermograms of TRG, f-TRGp, and f-TRGs. Samples were heated from 50-500° C at 10° /min under nitrogen

The electrical resistance of pure and functionalized TRG samples has been investigated using a custom made conductivity setup. The functionalization, as expected, has appeared to increase the resistance of graphene. The measured room temperature resistance of TRG of 42 ohms slightly increases to 50.8 ohms for f-TRG_P but increased significantly to 230 ohms for f-TRG_S. The increased resistance (decrease in conductivity) is expected due to the increase in sp^3-contents in the f-TRG_S as indicated by I_D/I_G ratio in the Raman spectra (see Figure 5). The edge distributed APTS in f-TRG_S seems to have a more pronounced effect on the conductivity compared to surface distributed groups in f-TRG_P. This may be due to the effect of the group distribution on the dispersion of sp^2-electronic cloud of TRG.

Conclusion

A simple catalyst-free method for synthesizing APTS-functionalized graphene was successfully demonstrated along with the effective role of organic solvent in directing the functionalities over the graphene surface and to the edges. The amount of APTS attached onto graphene was determined by XPS and TGA and the covalent linkages were confirmed by FTIR, XPS, EELS and Raman spectroscopy. TEM and EELS analyses show that no substantial change in surface morphology of graphene was observed upon APTS functionalization in solution whereas pure APTS appears to attack the sheets adversely and changed the morphology considerably.

The quantification of the f-TRG showed more than 7-8 atomic % attachment of Si, which is higher than any previously reported functionalization. The method of APTS intercalation/ incorporation has a significant effect on the structure and properties of the resulting functional material. Based on the EFTEM elemental mapping, it can be proposed that the selective end-functionalization can be achieved using a suitable solvent during the course of the silylation reaction. The f-TRG has shown good thermal stability over the temperature range of 50-500 °C where only 16% weight loss is observed for pure TRG compared to 22% for TRGp and ~25% for TRGs. The decrease in electrical conductivity (increase in electrical resistance) of TRG with functionalization has been attributed to the increase in sp3-contents. Further studies can evolve a better mechanism for selective functionalization of TRG with APTS.

Acknowledgements

The authors would like to thank Mr. Issam Ismail at the Department of Chemical Engineering and Materials Science, University of Minnesota for the XPS measurements, Kelly Mason at National Renewable Energy Laboratory (Golden, CO) for helping in the conductivity measurements, and Dr. Sunil Lonkar at the Department of Chemical Engineering, The Petroleum Institute for his valuable comments. This project has been supported by The Petroleum Institute in Abu Dhabi through the Cooperative Research Partnership with Colorado School of Mines.

Notes and references

[a] *Department of Chemical Engineering, The Petroleum Institute, PO Box 2533, Abu Dhabi, U.A.E. Fax: +971 2 6075200; Tel:+971 2 607 5584; E-mail: aabdala@pi.ac.ae*

[b] *Department of Chemical and Biological Engineering, Colorado School of Mines, Golden CO 80401, U.S.A.*

[c] *Department of Chemical Engineering and Petroleum Refining, Faculty of Petroleum and Mining Engineering, Suez University, Suez, Egypt*

† Electronic Supplementary Information (ESI) available: [Experimental details, XRD, TEM of TRG and EDS results are included in supplementary information.]. See DOI: 10.1039/b000000x/

1. K. Novoselov, A. Geim, S. Morozov, D. Jiang, Y. Zhang, S. Dubonos, I. Grigorieva and A. Firsov, *Science*, 2004, **306**, 666-669.
2. S. L. Cheekati, MS Thesis, Wright State University Dayton, Ohio, 2011.
3. A. Balandin, S. Ghosh, W. Bao, I. Calizo, D. Teweldebrhan, F. Miao and C. Lau, *Nano letters*, 2008, **8**, 902-907.
4. D. A. Dikin, S. Stankovich, E. J. Zimney, R. D. Piner, G. H. B. Dommett, G. Evmenenko, S. B. T. Nguyen and R. S. Ruoff, *Nature*, 2007, **448**, 457-460.
5. A. Geim and K. Novoselov, *Nature Materials*, 2007, **6**, 183-191.

6. T. Ramanathan, A. Abdala, S. Stankovich, D. Dikin, M. Herrera-Alonso, R. Piner, D. Adamson, H. Schniepp, X. Chen and R. Ruoff, *Nature Nanotechnology*, 2008, **3**, 327-331.
7. H. Pang, T. Chen, G. Zhang, B. Zeng and Z. Li, *Materials Letters*, 2010, **64**, 2226-2229.
8. T. Kuilla, S. Bhadra, D. Yao, N. Kim, S. Bose and J. Lee, *Progress in Polymer Science*, 2010, **35**, 1350-1375.
9. H. Kim, PhD Thesis, University of Minnesota, Minnesota, 2009.
10. H. Kim, A. Abdala and C. Macosko, *Macromolecules*, 2010, **43**, 6515-6530.
11. L. Schlapbach and A. Züttel, *Nature*, 2001, **414**, 353-358.
12. M. Iqbal and A. A. Abdala, *RSC Adv.*, 2013, **3**, 24455-24464.
13. M. Z. Iqbal and A. A. Abdala, *Environmental Science and Pollution Research*, 2012, **20**, 3271-3279.
14. F. Schedin, A. Geim, S. Morozov, E. Hill, P. Blake, M. Katsnelson and K. Novoselov, *Nature Materials*, 2007, **6**, 652-655.
15. V. Georgakilas, M. Otyepka, A. B. Bourlinos, V. Chandra, N. Kim, K. C. Kemp, P. Hobza, R. Zboril and K. S. Kim, *Chemical reviews*, 2012, **112**, 6156-6214.
16. P. Ma, J. Kim and B. Tang, *Carbon*, 2006, **44**, 3232-3238.
17. A. Shanmugharaj, J. Bae, K. Lee, W. Noh, S. Lee and S. Ryu, *Composites Science and Technology*, 2007, **67**, 1813-1822.
18. X. Wang, W. Xing, P. Zhang, L. Song, H. Yang and Y. Hu, *Composites Science and Technology*, 2012, **72**, 737-743.
19. H. Yang, F. Li, C. Shan, D. Han, Q. Zhang, L. Niu and A. Ivaska, *J. Mater. Chem.*, 2009, **19**, 4632-4638.
20. K. Yang and M. Gu, *Composites Part A: Applied Science and Manufacturing*, 2010, **41**, 215-221.
21. W. Gao, L. Alemany, L. Ci and P. Ajayan, *Nature Chemistry*, 2009, **1**, 403-408.
22. H. Gaspar, C. Pereira, S. Rebelo, M. Pereira, J. Figueiredo and C. Freire, *Carbon*, 2011, **49**, 3441-3453.
23. S. Ganguli, A. K. Roy and D. P. Anderson, *Carbon*, 2008, **46**, 806-817.
24. R. Prud'Homme, I. Aksay, D. Adamson and A. Abdala, US Patent 7,658,901, 2010.
25. L. Staudenmaier, *Ber. Dtsch. chem. Ges.*, 1898, **31**, 1481-1487.
26. M. Worch, H. J. Engelmann, W. Blum and E. Zschech, *Thin Solid Films*, 2002, **405**, 198-204.
27. A. Shanmugharaj, J. Bae, K. Y. Lee, W. H. Noh, S. H. Lee and S. H. Ryu, *Composites Science and Technology*, 2007, **67**, 1813-1822.
28. R. Waltman, J. Pacansky and C. Bates Jr, *Chemistry of Materials*, 1993, **5**, 1799-1804.
29. S. Y. Jing, H. J. Lee and C. K. Choi, *Journal of Korean Physcial Society*, 2002, **41**, 769-773.
30. S. Wakeland, R. Martinez, J. K. Grey and C. C. Luhrs, *Carbon*, **48**, 3463-3470.
31. S. Urbonaite, S. Wachtmeister, C. Mirguet, E. Coronel, W. Y. Zou, S. Csillag and G. Svensson, *Carbon*, 2007, **45**, 2047-2053.
32. A. Falqui, V. Serin, L. Calmels, E. Snoeck, A. Corrias and G. Ennas, *Journal of microscopy*, 2003, **210**, 80-88.
33. K. Giannakopoulos, N. Boukos and A. Travlos, *Superlattices and Microstructures*, 2006, **39**, 115-123.
34. L. Laffont, M. Monthioux, V. Serin, R. B. Mathur, C. Guimon and M. F. Guimon, *Carbon*, 2004, **42**, 2485-2494.
35. W. M. Skiff, R. W. Carpenter and S. H. Lin, *Journal of applied physics*, 1987, **62**, 2439-2449.
36. G. A. Botton and M. W. Phaneuf, *Micron*, 1999, **30**, 109-119.
37. G. J. Auchterlonie, D. R. McKenzie and D. J. H. Cockayne, *Ultramicroscopy*, 1989, **31**, 217-222.
38. S. BittoloáBon, *Journal of Materials Chemistry*, 2011, **21**, 3428-3431.
39. M. Pimenta, G. Dresselhaus, M. S. Dresselhaus, L. Cancado, A. Jorio and R. Saito, *Physical Chemistry Chemical Physics*, 2007, **9**, 1276-1290.
40. Y.-T. Liu, J.-M. Yang, X.-M. Xie and X.-Y. Ye, *Materials Chemistry and Physics*, 2011, **130**, 794-799.
41. D. Graf, F. Molitor, K. Ensslin, C. Stampfer, A. Jungen, C. Hierold and L. Wirtz, *Nano letters*, 2007, **7**, 238-242.
42. A. Ferrari, J. Meyer, V. Scardaci, C. Casiraghi, M. Lazzeri, F. Mauri, S. Piscanec, D. Jiang, K. Novoselov and S. Roth, *Physical review letters*, 2006, **97**, 187401.
43. K. N. Kudin, B. Ozbas, H. C. Schniepp, R. K. Prud'Homme, I. A. Aksay and R. Car, *Nano letters*, 2008, **8**, 36-41.
44. M. Fang, K. Wang, H. Lu, Y. Yang and S. Nutt, *Journal of Materials Chemistry*, 2010, **20**, 1982-1992.
45. M. Quintana, K. Spyrou, M. Grzelczak, W. R. Browne, P. Rudolf and M. Prato, *ACS nano*, 2010, **4**, 3527-3533.
46. Y.-S. He, P. Gao, J. Chen, X. Yang, X.-Z. Liao, J. Yang and Z.-F. Ma, *RSC Advances*, 2011, **1**, 958-960.
47. J. Clark and D. Macquarrie, *Chemical Communications*, 1998, 853-860.
48. A. Wight and M. Davis, *Chemical reviews*, 2002, **102**, 3589-3614.

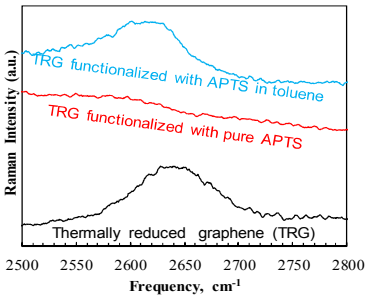

Toluene affects the distribution of APTS on the surface of thermally reduced graphene during the catalyst free silylation.